IOP Conference Series: Materials Science and Engineering

Research on hysteretic behavior of external T-stiffener box-column I-beam space connections

To cite this article: L Jin *et al* 2020 *IOP Conf. Ser.: Mater. Sci. Eng.* **789** 012030

IOP Conf. Series: Materials Science and Engineering **789** (2020) 012030 doi:10.1088/1757-899X/789/1/012030

Research on hysteretic behavior of external T-stiffener box-column I-beam space connections

L Jin[1], L P Chen[1] and Y Zhang[1*]

[1] School of Civil Engineering, Shenyang Jianzhu University, Shenyang, China

[*] ZY_JZDX@163.com

Abstract. The bearing capacity and deformation performance of external T-stiffener box-column to I-beam space connections were analyzed in this paper. A great deal of full-path analysis of space connections has been carried out by using finite element program ABAQUS with different parameters, which are box-column section width, I-beam flange width, section height of I-beam, flange width and web length of T- stiffener. FEM is proposed for numerical simulation under cycling loading based on the mechanical properties of materials. The result show that the hysteresis curve is the spindle shape and relatively full of T-stiffener box-column I-beam space connections. The ductility coefficient μ is larger than 4.0 and equivalent viscous damping coefficient h_e is larger than 0.2 of the space connections, which have been met the limitation of the specification requirements. The bearing capacity and deformation performance of external T-stiffener box-column I-beam space connections can be improved with the increasing of T- stiffener flange width and web length effectively. Due to the fine performance of ductility, energy dissipation and seismic performance, the external T-stiffener box-column I-beam space connections can be proposed used in multi-layer steel structure engineering widely.

1. The first section in your paper

Box-column for steel structures are generally welded by four steel plates [1], as shown in figure 1. Generally, in order to improve the lateral stiffness and torsion resistance of box-column, an internal partition is provided in the connection between box-column and I-beam at a corresponding position [2].

However, the actual welding process between the inner partition and the four steel plates is the greatest difficulty [3]. In view of the problem, the actual welding process is time-consuming, laborious and the quality of the weld is not guaranteed.

The external T-stiffener box-column I-beam connections can be used to avoid the welding difficulties of box-columns during welding [4-6]. The relevant research shows that the external reinforcement is simpler, faster and more economical than the traditional method of adding diaphragm in the column, and the T-external reinforcement connections have enough strength, rigidity and rotation capacity [7-9]. The T-stiffener box-column I-beam connections is shown in figure 2 [10-12].

At present, most of the researches are focused on plane connections, for empty connections the research of space connections is relatively few [13-14]. Due to the uncertainty of the direction of seismic force, the stress of the middle column joint is characterized by spatial stress. Therefore, in this paper, T-stiffener box-column I-beam space connections is selected for research, as shown in figure 3. The hysteretic behavior of spatial connections is studied by changing the parameters of box columns, I-beams and T-stiffeners.

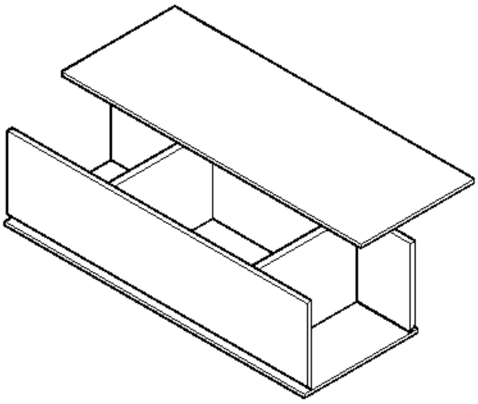

Figure 1. Box-column.

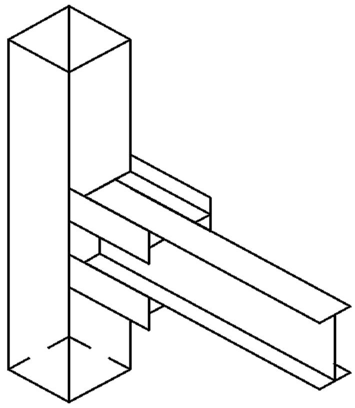

Figure 2. T-stiffener box-column I-beam connections.

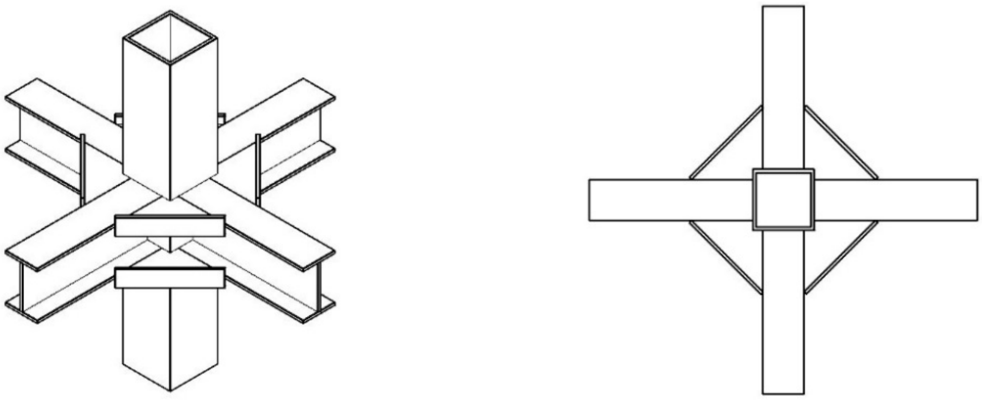

(a) Node axonometric drawing. (b) Node top view.

Figure 3. T-stiffener box-column I-beam space connections geometry model.

2. Finite element model

2.1. Connection design

The finite element program ABAQUS is used to build the modelling [15], the connection geometry model and loading method are shown in figure 4. Steel Q345B is selected and other properties of the material are shown in the table 1.

The constitutive relation is selected as a linear elastic elastoplastic mechanical model of double-fold line. The steel stress-strain relationship is shown in figure 5.

The external T-stiffener box-column I-beam space connections is referred to as ST in the following content. Eight kinds of working conditions for simulation analysis were designed. The working condition number is shown in figure 6.

Table 1. Mechanical properties [16].

material	Yield stress fy/MPa	Tensile strength (MPa)	Elasticity modulus (10^5MPa)	Poisson's ratio
Q345B	375.7	544.5	2.06	0.3
artifacts	Length of I-beam (mm)		Height of box column (mm)	
ST	1250		750 mm above and below each box column	

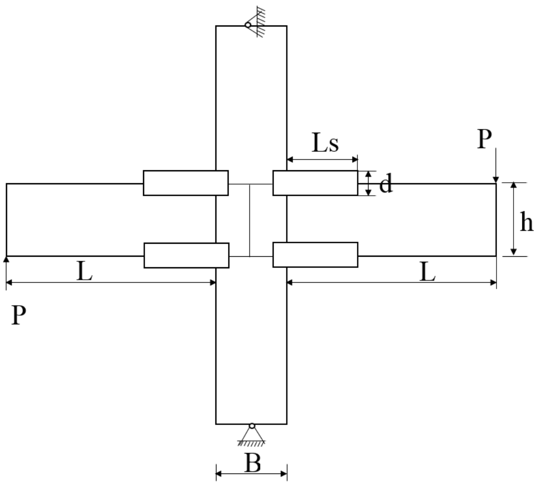

Figure 4. Geometry model and loading method.

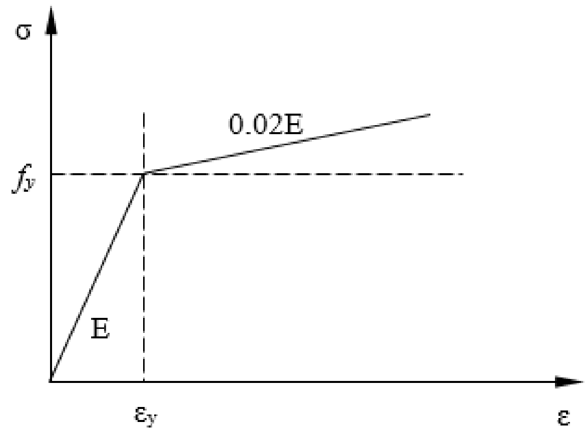

Figure 5. Steel stress-strain relationship.

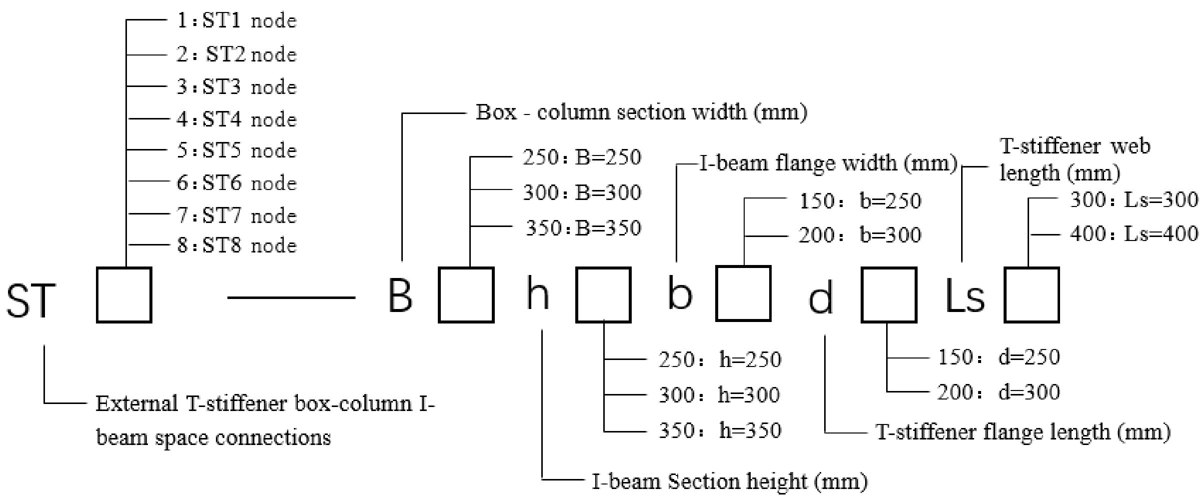

Figure 6. Working condition number.

2.2. Establishment of finite element model

According to table 1 dimensions of beams and columns, the numerical model of spatial connection is established, the T-stiffener box-column I-beam space connections finite element model is shown in figure 7.

The selection of mesh shape and global size of the finite element model will directly affect the calculation cost and accuracy of the calculation results. By comparison, when the overall dimensions of box column, I-beam and T-stiffener are 60 mm, 40 mm and 30 mm respectively, the calculation accuracy and calculation time are appropriate.

Tie restraint relationship were used between box column, I-beam and T-stiffener, reciprocating load is applied by displacement control at beam end [17-19].

Three stages of loading Δ/ 3, 2 Δ/ 3 and Δ before yield, one cycle per stage, after yielding, cycle three times for each stage according to 2 Δ, 3 Δ, 4 Δ, 5 Δ. The loading curve is shown in figure 8.

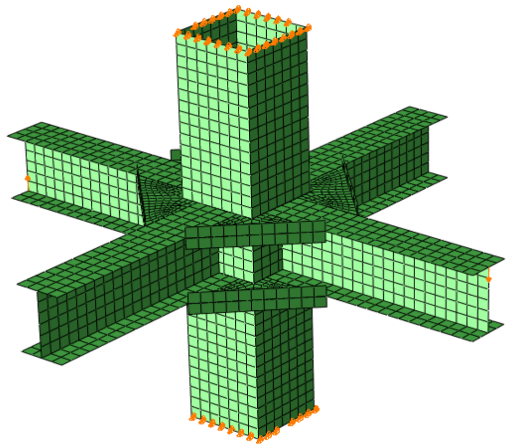

Figure 7. Finite element model.

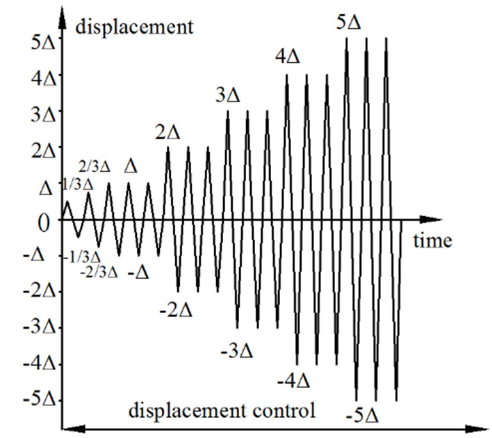

Figure 8. Typical cyclic loading sequence.

3. Hysteresis performance

3.1. Hysteresis curve

The numerical model was established refer to the above steel constitutive. The working condition design numbers of the 8 space connections are shown in table 2. The hysteresis curves of the end of beam is shown in figure 9.

Table 2. Design condition.

condition	number	condition	number
1	ST1-B250 h250 b150 d100 Ls300	2	ST2-B250 h350 b150 d100 Ls300
3	ST3-B300 h350 b200 d100 Ls300	4	ST4-B350 h300 b200 d100 Ls300
5	ST5-B350 h350 b200 d100 Ls300	6	ST6-B300 h350 b150 d100 Ls300
7	ST7-B300 h350 b200 d160 Ls300	8	ST8-B300 h350 b200 d100 Ls400

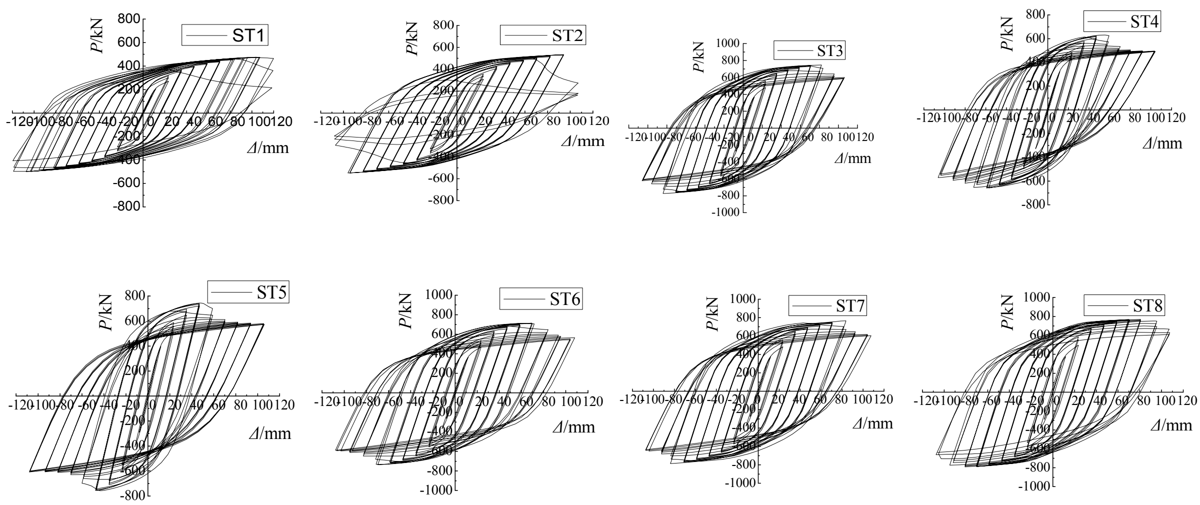

Figure 9. Hysteresis curves.

The result show that the beam and column dimensions of connection ST1 and ST2 are much smaller than others. As a result, its bearing capacity decreases, but its ductility increases. Connection ST1- ST8 has a decrease in stiffness under cyclic loading.

However, the hysteresis curve becomes fuller with the increasing of the cross-section width of the box column, the height of the I-beam and the length of the stiffener web. Hysteresis performance has been improved significantly.

3.2. Skeleton curve

The figure 10 represents the skeleton curves of the external T-stiffener box-column I-beam space connections. As shown in figure 10(a), with the section width of the box column increasing from 250 mm to 350 mm, the bearing capacity of connection ST6 is increased by 61.41% compared with connection ST2. The bearing capacity of connection ST5 is increased by 7.67% compared with connection ST3. As shown in figure 10(b), with the increasing of the height of the I-beam, the bearing capacity of connection ST2 is increased by 8.28% compared with connection ST1. The bearing capacity of connection ST5 is increased by 22.93% compared with connection ST4. As shown in figure 10(c) and figure 10(d), compared with connection ST3, the increasing of T-stiffeners' flange width and web length leads to the load capacity of connection ST7 and ST8 increase by 0.83% and 1.14%, respectively.

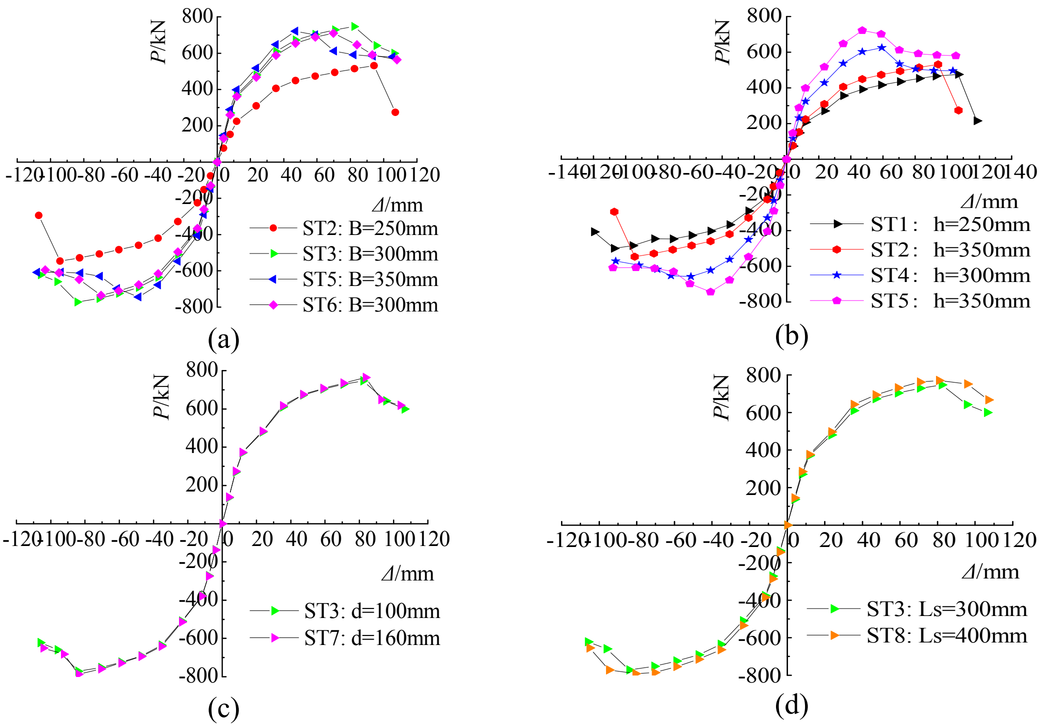

Figure 10. Skeleton curves.

3.3. Stiffness degradation

The figure 11 are the stiffness degradation curves of the external T-stiffener box-column I-beam space connections. As shown in the stiffness degradation curves and the table 3.

Since connection ST1 and connection ST2 are smaller size than others, it can be seen that the initial stiffness of the connection ST1 and ST2 is about 1.5 times lower than the initial stiffness of others as the same displacement. The stiffness of the connection ST5 is increased by 21.55% compared with connection ST4, the stiffness of the connection ST8 is 5.65% higher than that of connection ST3.

Increasing the section width of box column and the web length of T-stiffener can improve the stiffness of space connections effectively.

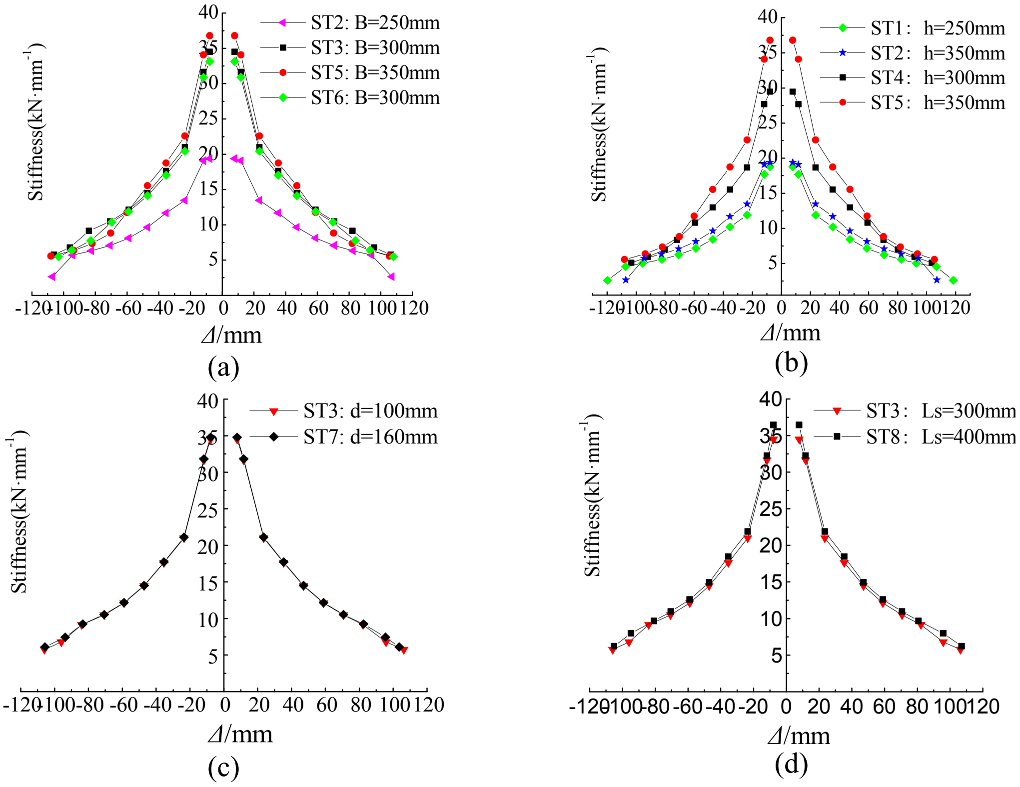

Figure 11. Stiffness degradation curves.

Table 3. Cyclic stiffness of each connection.

condition	Cyclic stiffness (N/mm)									
	K_1	K_2	K_3	K_4	K_5	K_6	K_7	K_8	K_9	K_{10}
ST1	18.774	17.686	11.903	10.212	8.428	7.149	6.238	5.576	5.041	2.611
ST2	19.385	19.083	13.467	11.679	9.637	8.120	7.076	6.319	5.717	2.655
ST3	34.503	31.639	20.984	17.615	14.466	12.117	10.476	9.143	6.793	5.756
ST4	29.452	27.684	18.663	15.525	12.983	10.812	8.351	6.990	5.952	5.091
ST5	35.798	34.075	22.592	18.743	15.542	11.761	8.832	7.340	6.362	5.575
ST6	33.136	30.897	20.437	17.025	14.118	11.863	10.368	7.753	6.391	5.488
ST7	34.947	31.908	21.176	17.790	14.528	12.190	10.568	9.272	7.186	6.090
ST8	36.431	32.261	21.882	18.476	14.933	12.596	10.957	9.668	7.988	6.232

3.4. Ductility

The calculation of the carrying capacity and ductility coefficient μ of the space connections ST1-ST8 and other performance indicators are shown in table 4.

With the increasing of flange width of T-stiffener from 100 mm to 160 mm and length of T-tiffener web from 300 mm to 400 mm, the space connections ductility coefficient increased by 5.69% and 3.09%. The ductility coefficient μ is larger than 4.0 of each condition and can meet the requirement of seismic specifications.

Table 4. Node carrying capacity and deformability.

Condition	Yield capacity Fy/kN	Yield displacement δy/mm	Ultimate capacity Fu/kN	Limit displacement δu/mm	Ductility coefficient μ
ST1	207.066	11.786	475.049	106.751	9.057
ST2	224.211	11.786	531.440	94.293	8.000
ST3	370.333	11.789	746.921	80.1413	6.797
ST4	324.351	11.785	625.164	59.306	5.032
ST5	398.732	11.782	721.154	47.345	4.018
ST6	361.889	11.786	710.112	69.818	5.924
ST7	373.416	11.785	764.652	84.659	7.184
ST8	375.536	11.786	769.999	80.771	6.853

3.5. Energy consumption

The equivalent viscous damping coefficient h_e and the energy dissipation coefficient E of the peak hysteresis loop of each condition are shown in table 5.

According to the energy dissipation coefficient E in the table 5, through the comparison of the two groups of connections ST2, ST6 and connections ST3, ST5. It can be seen that the energy consumption capacity of the enlarged box-column section width is increased by about 1.18% and 3.91% respectively. With the cross-section height of the I-beam increasing, for example, from connection ST1 to ST2, from connection ST4 to ST5, it can be seen that the energy consumption capacity is increased by 1.33% and 6.36% respectively.

Comparing the energy dissipation coefficient E of the connection ST3 and ST6, it is known that the energy consumption capacity of the flange of the I-beam is increased by 7.89%.

As shown in table 5, figure 12 and figure 13, connection ST3, ST7 and ST8, with increasing width of the flange of the T-stiffener and the length of the web of the T-stiffener, resulting in an increase in energy consumption of 2.59% and 6.79% respectively.

The equivalent viscous damping coefficient h_e of the eight space connections is larger than 0.2, indicating that this type of space connection can meet the requirements of seismic design energy performance.

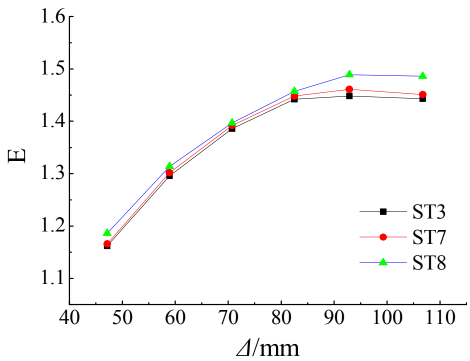

Figure 12. E-displacement curves.

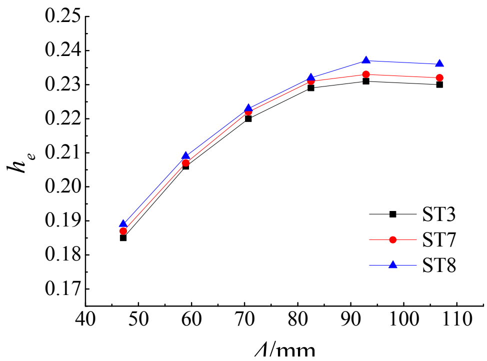

Figure 13. h_e-displacement curves.

Table 5. Energy dissipation coefficients.

Dissipation coefficient	ST1	ST2	ST3	ST4	ST5	ST6	ST7	ST8
h_e	0.240	0.263	0.230	0.223	0.237	0.246	0.231	0.237

E	1.508	1.528	1.443	1.400	1.489	1.546	1.461	1.486

Conclusions

The performance of the external T-stiffener box-column I-beam space connections have been studied. The research focuses on the influence of changing the section width of the box column, the width of the I-beam flange, the height of the section, the width of the T-stiffener flange and the length of the web on the bearing capacity and deformation performance. The following conclusions are got:

- the hysteresis curves of the T-stiffener box-column I-beam space connections are the full spindle shape. The performance of deformation is strong in the elastoplastic stage;
- the ductility coefficient μ of the space joints with T-stiffener is larger than 4.0 and meets the requirement of seismic specifications;
- the stiffness decreases significantly with the increasing of the displacement. The rate of descent has a rapid decrease followed by a slow decrease.
- The equivalent viscous damping coefficient h_e is larger than 0.2 and energy dissipation coefficient E is larger than 1.4.

Acknowledgement

The work presented in this paper was supported by the natural foundation guidance program of Liaoning province, China (2019-ZD-0678) and the program for “Xing Liao Talent” of Liaoning province, China (XLYC1807188).

References

[1] Mao H Jia B L and Bu Y 2011 *J. Electric Welding Machine* **41** pp 53-57
[2] Deylami A and Gholipou R M 2011 *J. Procedia Engineering* **2011** pp 3252-3259
[3] Zhao X B, Zheng Z K and Pan J F 2016 *J. Steel Construction* **31** pp 92-95
[4] Wang Y, Liu Y, Wang P and Gao P 2011 *J. Progress in Steel Building Structures* **13** pp 1-7
[5] Shanmugam N E 1997 *J. Journal of Structures* **17** pp 36-60
[6] Shanmugam N E and Ting L C 1995 *J. Journal of Structural Engineering* **121** pp 824-830
[7] Yang X D 2011 *D. Xian University of Architecture and Technology*
[8] Nia Z S, Mazroi A, Ghassemieh M and Pezeshki H 2014 *J. Earthq Eng & Eng Vib* **13** pp 717-29
[9] Kato B 2014 *J. Journal of the Structure Division* **108** pp 343-360
[10] Wang M, Shi Y and Wang Y 2013 *J. Constructional Steel Research* **90** pp 140-152
[11] Mirghaderi S R, Torabian S and Keshavarzi F 2011 *J. Engineering structures* **2011** pp 2034-2048
[12] Jin L 2006 *D. Harbin Institute of Technology*
[13] Shao Y S, Jin L, Xie L L and Zhang Y C 2009 *J. Journal of Harbin Institute of Technology* **41** pp 20-25
[14] Li F X and Wang X W 2018 *J. Steel Construction* **33** pp 98-102
[15] Xu P Z, Yang L, Zhu Y G and Jing H K 2018 *J. Steel Construction* **33** pp 93-97
[16] Zhang Z X 2015 *D. China University of Mining and Technology*
[17] Liu E H 2017 *D. Chang an University*
[18] Wei K F, Li J F, Liu S X, Li X and Chen H 2018 *J. Steel Construction* **33** pp 17-20
[19] Xu Z G, Zhang Z B and Deng C G 2017 *J. Sichuan Building Science* **43** pp 75-79